Available online at www.sciencedirect.com
SCIENCE DIRECT®
Journal of Molecular Graphics and Modelling 23 (2005) 433–438
Journal of Molecular Graphics and Modelling
www.elsevier.com/locate/JMGM

Modeling kinase–substrate specificity: implication of the distance between substrate nucleophilic oxygen and attacked phosphorus of ATP analog on binding affinity

Ming Sun[a,b,1], Xiao-Hong Liu[a,1], San-Hao Ji[a], Yu-Fen Zhao[a,*]

[a]*The Key Laboratory of Phosphorous Chemistry and Chemical Biology of Ministry of Education, Department of Chemistry, Tsinghua University, Beijing 100084, China*
[b]*School of Chemistry and Life Science, Tianjin Normal University, Tianjin 300074, China*

Received 23 December 2003; received in revised form 17 December 2004; accepted 17 December 2004
Available online 20 January 2005

Abstract

Molecular dynamics simulations were performed on modeled kinase–substrate complexes in an attempt to establish a relationship between structural features and binding ability of the complexes. We found that the monitored distance between substrate nucleophilic oxygen (OG) and attacked phosphorus (PG) of ATP analog correlated closely with the binding affinity. With reference to 3.3 Å, the van der Waals sum of oxygen and phosphorus, the calculated distances of good substrates were close to it whereas those of poor substrates were far apart from it. Therefore, it is reasonable to consider the OG–PG distance as a potential criterion to prefigure the kinase–substrate binding specificity and the simple computational techniques may work as an easy approach to distinguish good substrates from weak or poor substrates.

Keywords: Kinase–substrate specificity; Distance; Binding affinity; Molecular dynamics simulation

1. Introduction

Protein kinases play a critical role in cell signaling pathways by catalyzing the transfer of the γ-phosphoryl group from ATP to the hydroxyl group of substrate side chain [1]. This process affects essentially every cellular process including metabolism, growth, differentiation, motility, membrane transport, learning and memory. To ensure the signaling fidelity, the kinases must be specific and act only on a defined subset of cellular targets. Therefore, understanding the basis of this substrate specificity of different protein kinases is essential. However, experimental approaches to determine the specificity are expensive and laborious and there are a large number of different kinases in the eukaryotic proteomes; therefore, it is impractical to determine the specificity of each enzyme experimentally.

The development of applicable techniques to study the substrate preference of protein kinases has made progress [2–5]. The possibility of discriminating potential substrates from non-substrates by simple computational techniques is attracting more attention recently. Järv and co-workers made a statistical analysis on the structural aspects of kinase–substrate specificity [6]. Their results indicate that the protein kinases belong to a group of enzymes which have rather a broad specificity, that on the other hand should be rigid enough to provide the necessary precision of targeting and selectivity of the regulatory phosphorylation phenomena. Kobe and co-workers analyzed the binding enthalpies of modeled enzyme–substrate complexes and correlated them with the experimental enzyme kinetic measurements [7]. Their results show that the computed enthalpies do not correlate closely with the kinetic measurements but the method can successfully distinguish good substrates from weak substrates and non-substrates.

* Corresponding author. Tel.: +86 10 62772259; fax: +86 10 62781695.
E-mail addresses: sunm@sun5.ibp.ac.cn (M. Sun), tp-dch@mails.tsinghua.edu.cn (Y.-F. Zhao).
[1] Authors equally contributed to this work.

1093-3263/$ – see front matter © 2004 Elsevier Inc. All rights reserved.
doi:10.1016/j.jmgm.2004.12.003

Protein kinases follow ternary complex kinetic mechanism in which direct transfer of the γ-phosphoryl group from ATP to protein substrate occurs [8,9]. The reaction mechanism of phosphoryl transfer reactions can favor either an associative pathway that involves a pentacoordinate phosphorus intermediate or dissociative pathway with a triganal planar metaphosphate intermediate [10]. The existence of both pentacoordinate phosphorus intermediate and metaphosphate intermediate has been substantiated by experimental or theoretical methods [11–17]. Our previous studies on *N*-phosphoryl amino acid have also proved that many biomimetic reactions preceded through a pentacoordinate phosphorus intermediate [18–22]. Although the nature of the transition state in the phosphoryl transfer reaction has been the subject of long-standing controversy, interatomic separation of a nucleophilic oxygen in a substrate and the phosphorus of ATP is obviously an important factor for the transfer of the phosphoryl group from ATP to protein substrate [23,24] and may be used as an indicator of possible enzymatic activity of the complex. The distance should be within the reference data 3.3 Å, the van der Waals sum of oxygen and phosphorus and be favorable for the substrate nucleophilic oxygen (OG) touching down to the phosphorus (PG) of ATP. In this study, we mainly focus on computing the OG–PG distances of modeled kinase–substrate complexes and correlating the OG–PG distances with the experimental enzyme kinetic measurements.

2. Methodology

All molecular modeling studies were performed on a Silicon Graphics O2 computer running InsightII [25] or Sybyl [26].

2.1. Protein data bank (PDB) based data mining

Protein date bank [27] was searched with keywords ''kinase and complex''. Homoserine kinase (HSK) [28] does not belong to protein kinase, so it is excluded from the selected set. The crystal structures of the other five kinases, which have been determined in ternary complexes with ATP (or analog) and inhibitor (or substrate peptides), were selected. These include cyclic AMP-dependent protein kinase A (PKA) [29], protein kinase Akt/PKB [30], insulin receptor tyrosine kinase (IRK) [31] and phosphorylase kinase (PHK) [32]. Superimposing was made by fitting corresponding atoms of ATP and OG in these known crystal structures using Fit module in Sybyl.

2.2. Molecular dynamic simulations on modeled enzyme–substrate complexes

The crystal structures of PHK (PDB ID: 2PHK) and cAMP-dependent PKA (PDB ID: 1ATP) were used as starting points to model various peptide complexes. The reason of choosing these two structures for testing the computational approach is that a series of peptides with enzyme kinetics results are available for both the kinases. For PHK, the substrate peptide RQMSFRL in crystal was used as a platform to build KQISVRG and the extended peptides KRKQISVRGL and variations. For PKA, the coordinates of the heptapeptide fragment ^{17}GRRNAIH^{23} from PKI in crystal were used to model LRRASLG and variations. In this way, the original substrate in crystal was replaced by a series of peptides with known assay data.

Because the peptide series chosen contained subtle modifications in individual substrate residues, it was reasonable to assume that the backbone atoms of all the peptides retained a similar binding mode. No formal docking of the substrates was, therefore, performed. The basic modeling methodologies leading to the energy-minimized complexes and molecular dynamic (MD) trajectories were performed using the CVFF molecular mechanics force field by Discover_3 module implemented in InsightII with a dielectric constant of 4 *r* and a 20 Å cutoff to compute the non-bonded interactions. Energy minimization was performed using the standard, steepest, decent and conjugate gradients minimization algorithms implemented in the program, leaving the complete structure free to relax. For MD, the peptide substrate together with the amino acids within 8 Å of the substrate were allowed for relaxation; the residues beyond this distance and the two Mn^{2+} cations were held frozen. ATP molecule was constrained by applying a default tether constant meanwhile. The assembly of amino acid residues allowed to relax was dynamically recalculated during the MD trajectory. After an initial 5 ps period of heating, MD was performed at 300 K with an integration step of 1 fs for 100 ps until the monitored OG–PG distance and the correspondent potential energy was relatively stable. Samples were taken at 1 ps intervals, yielding 100 conformation frames for analysis. The possible correlation between monitored OG–PG distances of last 50 frames and kinetic measurements of the series of modeled enzyme–peptide complexes was particularly studied here.

3. Results and discussion

3.1. Protein data bank based data mining

The distances between substrate OG and attacked PG of ATP analogs in the six ternary complexes are summarized in

Table 1
Summary of OG–PG distances in kinase ternary complexes

Protein	PDB ID	OG–PG distance (Å)
cAMP-dependent protein kinase A	1ATP	3.66
cAMP-dependent protein kinase B	1O6K	3.57
	1O6L	3.54
Insulin receptor tyrosine kinase (IRK)	1IR3	5.08
Phosphorylase kinase (PHK)	2PHK	3.61

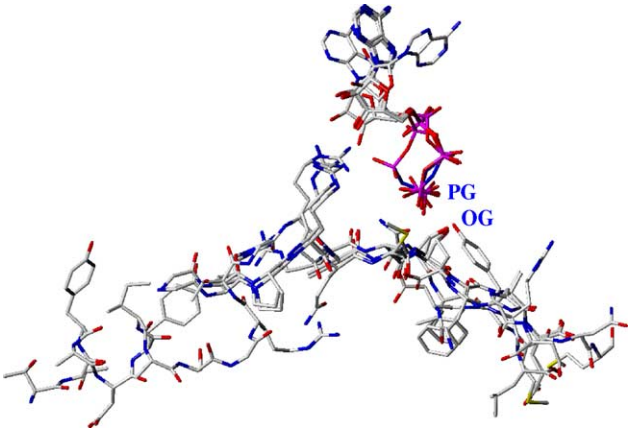

Fig. 1. The overlap map of the binding structures of ATP (analog) and substrate abstracted from the five ternary kinase complexes: 1ATP, 1O6K, 1O6L, 1IR3, 2PHK.

Table 1. The overlap map of the binding structures of ATP (analog) and substrate abstracted from these six complexes is shown in Fig. 1.

It is obvious that the OG–PG distances in most of these ternary complexes are in the range of 3.4–3.7 Å. The longer distance in 1IR3 (5.08 Å) may be attributed to the larger volume of Tyr side chain or different mechanics [9,30]. If we take 3.3 Å, the van der Waals sum of oxygen (1.4 Å) and phosphorus (1.9 Å), as a reference, it may be deduced that the distance from the nucleophilic oxygen of a good substrate to the γ-phosphoryl group of ATP should be within a contactable distance. The overlap map also exhibits that the structures of the active kinases display a similar conformation in the key region involved in ATP and substrate recognition. The recognition pattern for different kinases is similar. Therefore, it is reasonable to choose the OG–PG distance as a potential criterion to predict kinase–substrate specificity.

3.2. Molecular dynamic simulations

For PHK, the Michaelis–Menten kinetic parameters for PHKγ_t with different peptide substrates and MD-simulated OG–PG average distances of the last 50 frames are summarized in Table 2. MD trajectories of the monitored OG–PG distances in the modeled ternary complexes are shown in Fig. 2. For cAMP-dependent protein kinase (PDB ID: 1ATP), the Michaelis–Menten kinetic parameters for PKA with different peptide substrates and MD-simulated OG–PG average distance are summarized in Table 3. MD trajectories of the monitored OG–PG distance in the modeled ternary complexes are shown in Fig. 3.

Because the OG–PG distances were monitored after only 1 ps MD simulation time, it was reasonable that the distances shifted sharply at first. The simulations were stopped after 100 ps when the monitored distance and potential energy were relatively stable.

Table 2
Kinetic characterizations and calculations of OG–PG distances of simulated peptides bound to PHK

Peptide[a]	K_m (mM) [5]	OG–PG distance (Å)[b]
1. Lys-Ala-Ala-Gln-Ile-**Ser**-Val-Arg-Gly-Leu	1.7 [36]	4.2
2. Lys-Arg-Lys-Gln-Ile-**Ser**-Val-Ala-Gly-Leu	2.5 [36]	4.6
3. Lys-Gln-Ile-**Ser**-Val-Arg-Gly[c]	1.8	4.0
4. Lys-Arg-Lys-Gln-Ile-**Ser**-Val-Arg-Gly-Leu[d]	0.9	3.7
5. Lys-Arg-Lys-Gln-Gly-**Ser**-Val-Arg-Gly-Leu	0.8	3.6
6. Lys-Ala-Lys-Gln-Ile-**Ser**-Val-Arg-Gly-Leu	0.9	3.6
7. Lys-Arg-Ala-Gln-Ile-**Ser**-Val-Arg-Gly-Leu	0.9	3.8

[a] Phosphorylation sites are shown in bold and substitutions from the parent peptide are underlined.
[b] The average distance of the last 50 frames.
[c] Corresponds to residues 11–17 of human glycogen phosphorylase GPb.
[d] Corresponds to residues 9–18 of human glycogen phosphorylase GPb.

For PHK, the monitored average distances for the five different peptides are within the range of 3.6–4.0 Å. They are all close to the van der Waals sum of oxygen and phosphorus (3.3 Å) and in appropriate distance values for the substrate OG touching down to the PG of ATP analogs. It informs us that the tested peptides might be relatively good substrates for PHK. This assumption is supported by the low K_m values of the peptides. The longest distance in complex of peptide 1 (4.0 Å) corresponds to a highest kinetic value (1.8 Mm) whereas the shortest distance in complex of peptide 3 (3.6 Å) corresponds to a lowest kinetic value (0.8 Mm). It may deduced that the shorter the distance, the higher the affinity. Unfortunately, the tested peptides have similar K_m values and it is hard to conclude that there is obvious correlation between the calculated distances and K_m values from this set of tested peptides. For PKA, peptide 2 with the smallest K_m value of 10.5 μM provides the shortest average OG–PG distance of 3.8 Å in our calculations which is close to 3.3 Å. Peptides 1, 3, and 4, which are relatively good substrates, also show contactable distances. Whereas in the case of weak substrate peptide 5 with a higher K_m value of 6300 μM, the monitored average OG–PG distance reaches to 4.6 Å which is much longer than 3.3 Å. For poor substrate peptide 6, the calculated average OG–PG distance exhibits the longest value of 7.2 Å. It can be deduced that the monitored distances correlate closely with the binding affinity. The binding affinity may lessen as the distance becomes longer. Therefore, by monitoring the separation of the reacting species, the simple computational method may work as an easy approach to distinguish good substrates from weak or non-substrates.

The reason of this correlation, with the fact that protein kinase–substrate recognition is achieved through marked complementarity of shape, hydropathy and electrostatic potential [32–35], may be that the specificity determination residues of the good substrate anchor the peptide in a catalytical productive conformation. In poor substrates, the unfavorable side chains force the peptide in a less optimal conformation and alternatively fail to lock the peptide to the

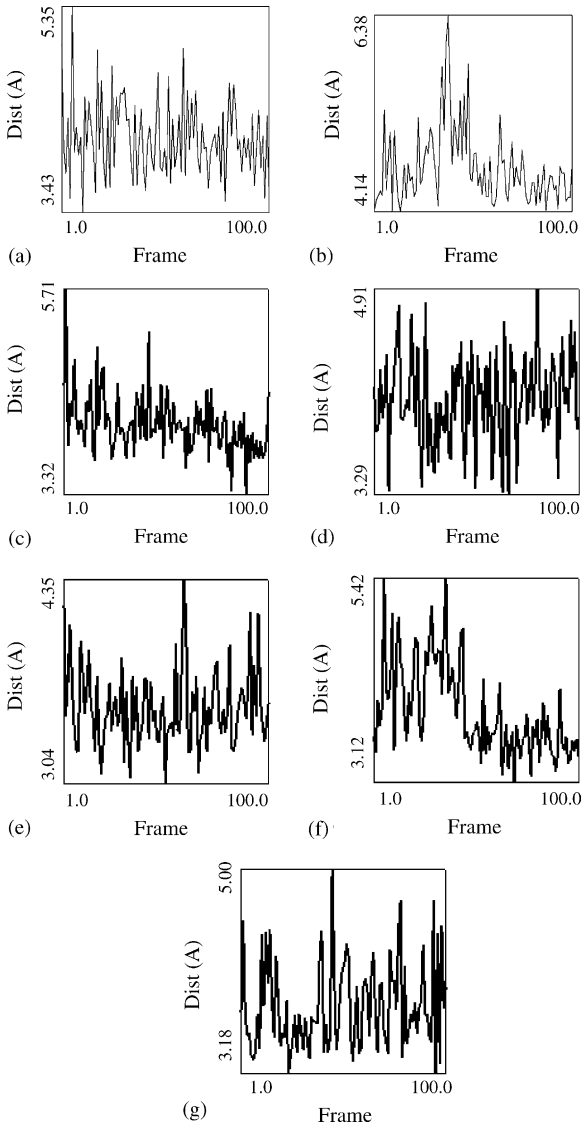

Fig. 2. Results of the molecular dynamics simulations. Graphics show plots of the monitored OG–PG distances in the ternary complexes of: (a) PHK with peptide 1, (b) PHK with peptide 2, (c) PHK with peptide 3, (d) PHK with peptide 4, (e) PHK with peptide 5, (f) PHK with peptide 6, and (g) PHK with peptide 7.

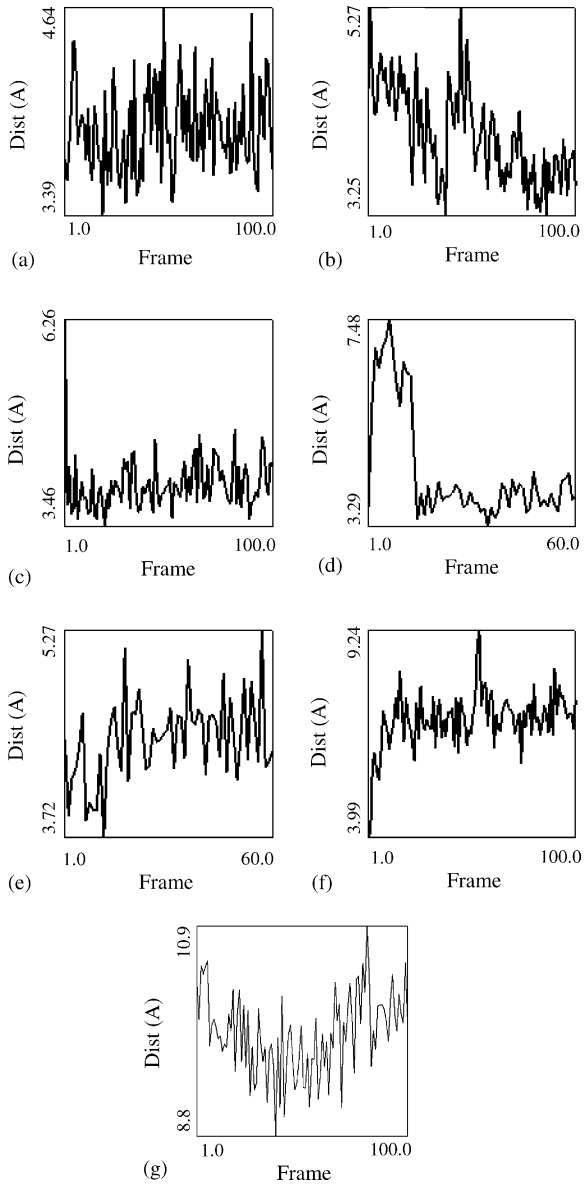

Fig. 3. Results of the molecular dynamics simulations. Graphics show plots of the monitored OG–PG distance in the ternary complex of: (a) PKA with peptide 1, (b) PKA with peptide 2, (c) PKA with peptide 3, (d) PKA with peptide 4, (e) PKA with peptide 5, (f) PKA with peptide 6, (g) PHK with peptide 7.

Table 3
Kinetic characterization and calculations of OG–PG distance of simulated peptides bound to PKA

Peptide[a]	K_m (μM) [7]	OG–PG distance (Å)[b]
1. Leu-Arg-Arg-Ala-**Ser**-Leu-Gly[c]	13.8	3.9
2. Leu-Arg-Arg-Gly-**Ser**-Leu-Gly	10.5	3.8
3. Leu-Arg-Arg-Trp-**Ser**-Leu-Gly	30	4.1
4. Leu-Lys-Arg-Ala-**Ser**-Leu-Gly	1400	3.9
5. Leu-Arg-Ala-Ala-**Ser**-Leu-Gly	6300	4.6
6. Leu-Arg-Arg-Ala-**Ser**-Gly-Gly	Poor substrate	7.2
7. Arg-Ala-**Ser**-Leu-Gly	4400 [36]	9.8

[a] Phosphorylation sites are shown in bold and substitutions from the parent peptide are underlined.
[b] The average distance of the last 50 frames.
[c] Corresponds to residues 1–7 of bovine pyruvate kinase.

kinase; thus on the average, the distance increases in the simulation. The OG–PG distance may only work as a simple expression of reflecting this complicated kinase–substrate specificity.

It can be concluded from examining the crystal structure of PHK (PDB ID: 2PHK) [31] that the major interactions involved in kinase and peptide substrate recognition are polar contacts and apolar contacts (Table 4).

Polar contacts are mainly those between Arg (−3) and Glu110, Gln (−2) and Ser188, Arg (+2) and Glu 182, anti-parallel β-sheet formed by Phe (+1) and Leu (+3) peptides with Gly185 and Val 183 from the enzyme through H-bonds.

Table 4
Major interactions between PHK and the peptide in crystal structure [32]

Pocket	Peptide residue	Major contacts <3.5 Å
(−3)	Arg	Glu110
(−2)	Glu	Ser188
(−1)	Met	–
(+1)	Phe	Val183, Pro187, Leu190
(+2)	Arg	Glu182
(+3)	Leu	Val183

The major apolar interaction involves Phe (+1), which sits in a hydrophobic pocket formed by Val 183, Pro187 and Leu 190 from the enzyme, together with Leu (+3) from the peptide substrate and itself interacts with this same apolar pocket. Our molecular dynamics simulations reveal that the interactions between PHK and tested peptide substrates are similar to those in the crystal structure. This may be because that the residues involved in the major interactions above only conduct subtle modifications. The substitution of Phe (+1) by Val exhibits little effect on the apolar interactions between kinase and peptides, and the substitution of Arg (−3) by Lys does not interfere with the polar interaction obviously either. As a result, the monitored OG–PG distances of tested peptides do not change obviously. And the substitution of Leu (+3) which can anchor the peptide in a catalytical productive conformation with apolar interaction by Gly fails to lock the peptide to the kinase; thus, on the average the OG–PG distance increases obviously.

The examination of the crystal structure of PKA (PDB ID: 1ATP) suggests that the major polar contacts between kinase and peptide substrate are mainly those between Arg (−3) and Glu 127, Arg (−2) and Glu 230. The major apolar interactions involve Ile (+1) which sits in a hydrophobic pocket formed by Phe 187, Pro 202, Leu 205, Ile 209 from the enzyme (Table 5). Therefore, the contributions for interaction made by Arg (−3), Arg (−2) and Ile (+1) to the overall complex are much more important than other residues of the substrate peptide. When Arg (−2) is replaced by Ala in peptide 5 and Ile (+1) is replaced by Gly in peptide 6, our calculations provide long OG–PG distances, suggesting that peptides 5 and 6 are both bad substrates. The results are in agreement with their low binding activities.

Table 5
Major interactions between PKA and the peptide in crystal structure [28]

Pocket	Peptide residue	Major contacts <3.5 Å
(−3)	Arg	Glu127
(−2)	Arg	Glu230
(−1)	Asn	–
(+1)	Ile	Phe187, Pro202, Leu205, Ile209
(+2)	His	–
(+3)	Asp	–

4. Conclusion

In the present work, we have established the relationship between the OG–PG distance and the kinetic measurements. The distance can be looked as a simple expression reflecting the complicated kinase–ATP–substrate ternary complex interaction. With reference to 3.3 Å, the van der Waals sum of oxygen and phosphorus, we show that the OG–PG distances for good substrates are close to this value whereas the OG–PG distances for poor substrates are much longer than that. The method may work as an easy approach to distinguish good substrates from weak or poor substrates.

Acknowledgements

We thank the financial supports from the Chinese National Natural Science Foundation (No. 20132020 and No. 20175026), The Ministry of Science and Technology, The Chinese Ministry of Education and Tsinghua University, and The Tianjin Science Foundation (No. 023606511).

References

[1] T. Hunter, Signaling 2000 and beyond, Cell 100 (2000) 113–127.
[2] Z. Songyang, L. Carraway Kermit III, J.E. Michael, et al. Catalytic specificity of protein-tyrosine kinases is critical for selective signaling, Nature 373 (1995) 536–539.
[3] B.E. Kemp, R.B. Pearson, Protein kinase recognition sequence motifs, Trends Biochem. Sci. 15 (1990) 342–346.
[4] Z. Songyang, S. Blechner, N. Hoagland, M.F. Hoekstra, H. Piwnica-Worms, L.C. Cantley, Use of an oriented peptide library to determine the optimal substrates of protein kinases, Curr. Biol. 4 (1994) 937–982.
[5] G.W. Tessmer, J.R. Skuster, L.B. Tabatabai, D.J. Graves, Studies on the specificity of phosphorylase kinase using peptide substrates, J. Biol. Chem. 252 (1977) 5666–5671.
[6] A. Kreegipuu, N. Blom, S. Brunakb, J. Järv, Statistical analysis of protein kinase specificity determinants, FEBS Lett. 430 (1998) 45–50.
[7] R.I. Brinkworth, J. Horne, B. Kobe, A computational analysis of substrate binding strength by phosphorylase kinase and protein kinase A, J. Mol. Recognit. 15 (2002) 104–111.
[8] M. Ho, H.N. Bramson, D.E. Hansen, J.R. Knowles, E.T. Kaiser, Stereochemical course of the phospho group transfer catalyzed by cAMP-depentent protein kinase, J. Am. Chem. Soc. 110 (1988) 2680–2681.
[9] K. Parang, J.H. Till, A.J. Ablooglu, R.A. Kohanski, S.R. Hubbard, P.A. Cole, Mechanism-based design of a protein kinase I inhibitor, Nat. Struct. Biol. 8 (2001) 37–40.
[10] J.R. Knowles, Enzyme-catalyzed phosphoryl transfer reactions, Annu. Rev. Biochem. 49 (1980) 877–919.
[11] K. Kim, P.A. Cole, Measurement of a BrØnsted nucleophile coefficient and insight into the transition state for a protein tyrosine kinase, J. Am. Chem. Soc. 119 (1997) 11096–11097.
[12] E. Skordalakes, G.G. Dodson, D.S.C. Green, C.A. Goodwin, M.F. Scully, H.R. Hudson, V.V. Kakkar, J.J. Deadman, Inhibition of human α-thrombin by a phosphonate tripeptide proceeds via a metastable pentacoordinated phosphorus intermediate, J. Mol. Biol. 311 (2001) 549–555.

[13] K. Kaur, M.J.K. Lan, R.F. Pratt, Mechanism of inhibition of the class C β-lactamase of enterobacter cloacae P99 by cyclic acyl phosph(o-n)ates: rescue by return, J. Am. Chem. Soc. 123 (2001) 10436–10443.
[14] T. Katagi, MNDO-PM3 study on gas-phase alkaline hydrolysis of phosphoryl and thiophosphoryl fluorides, J. Mol. Struct. (Theochem.) 538 (2001) 157–164.
[15] A.J. Ablooglu, J.H. Till, K. Kimi, K. Parangi, P.A. Cole, S.R. Hubbard, R.A. Kohanski, Probing the catalytic mechanism of the insulin receptor kinase with a tetrafluorotyrosine-containing peptide substrate, J. Biol. Chem. 275 (2000) 30394–30398.
[16] A. Cook, E.D. Lowe, E.D. Chrysina, V.T. Skamnaki, N.G. Oikonomakos, L.N. Johnson, Structural studies on phospho-CDK2/cyclin A bound to nitrate, a transition state analogue: implications for the protein kinase mechanism, Biochemistry 41 (2002) 7301–7311.
[17] J.P. Abrahams, A.G.W. Leslie, R. Luter, J.E. Walker, Structure at 0.28 nm resolution of F1-ATPase from bovine mitochondria, Nature 370 (1994) 621–628.
[18] H. Fu, Z.L. Li, Y.F. Zhao, G.Z. Tu, Oligomerization of *N*,*O*-bis(trimethylsilyl)-α-amino acid into peptides mediated by *o*-phenylene phosphorochoridate, J. Am. Chem. Soc. 121 (1999) 291–295.
[19] Z.Z. Chen, Y.M. Li, J. Ma, B. Tan, S. Inagaki, Y.F. Zhao, Activations of α-COOH vs γ-COON in *N*-phosphoryl amino acids: a theoretical study, J. Phys. Chem. A 106 (2002) 11565–11569.
[20] C.X. Lin, Y.M. Li, C.M. Cheng, B. Han, R. Wan, Y.B. Feng, Y.F. Zhao, Penta-coordinate phosphorous compounds and biochemistry, Sci. Chin. B45 (2002) 337–348.
[21] Z. Liu, L. Yu, Y. Chen, N. Zhou, J. Chen, C.J. Zhu, B. Xin, Y.F. Zhao, Interesting differences between the protonated and sodium adducts of pentacoordinated bisaminoacylspirophosphoranes in electrospray ionization mass spectrometry, J. Mass Spectrom. 38 (2002) 231–233.
[22] H. Fu, J.H. Xu, R.J. Wang, Z.Z. Chen, G.Z. Tu, Q.Z. Wang, Y.F. Zhao, Synthesis, crystal structure and diastereomeric transfer of pentacoordinated phosphoranes containing valine or iso-leucine residue, Phosphorus, Sulfur Silicon Relat. Elem. 178 (2003) 1963–1971.
[23] A.S. Mildvan, D.C. Fry, NMR studies of mechanism of enzyme action, Adv. Enzymol. Relat. Areas Mol. Biol. 59 (1987) 241–313.
[24] A.S. Mildvan, Mechanisms of signaling and related enzymes, Proteins: Struct. Funct. Genet. 29 (1997) 401–416.
[25] InsightII, Version 2000.1, Molecular Simulations Inc., San Diego, CA.
[26] Sybyl, Version 6.7, Tripos Associates, St. Louis, MO.
[27] The Protein Data Bank (PDB), The Research Collaboratory for Structural Bioinformatics, Rutgers, NJ, http://www.rcsb.org/pdb.
[28] S. Sri Krishna, T. Zhou, M. Daugherty, A. Osterman, H. Zhang, Structural basis for the catalysis and substrate specificity of homoserine kinase, Biochemistry 40 (2001) 10810–10818.
[29] J. Zheng, E.A. Trafny, D.R. Knighton, N. Xuong, S.S. Taylor, E.L.F. Ten Eyck, J.M. Sowadski, 2.2-Angstrom refined crystal-structure of the catalytic subunit of cAMP-dependent protein-kinase complexed with MnATP and a peptide inhibitor, Acta Crystallogr. D49 (1993) 362–365.
[30] J. Yang, P. Cron, V.M. Good, V. Thompson, B.A. Hemmings, D. Barford, Crystal structure of an activated Akt/protein kinase B ternary with GSK3-peptide and AMP-PNP, Nat. Struct. Biol. 9 (2002) 940–944.
[31] S.R. Hubbard, Crystal structure of the activated insulin receptor tyrosine kinase in complex with peptide substrate and ATP analog, EMBO J. 16 (1997) 5573–5581.
[32] E.D. Lowe, M.E. Noble, V.T. Skamnaki, N.G. Oikonomakos, D.J. Owen, L.N. Johnson, The crystal structure of a phosphorylase kinase peptide substrate complex: kinase substrate recognition, EMBO J. 16 (1997) 6646–6658.
[33] L.N. Johnson, E.D. Lowe, M.E. Noble, D.J. Owen, The structural basis for substrate recognition and control by protein kinases, FEBS Lett. 430 (1998) 1–11.
[34] R.I. Brinkworth, R.A. Breinl, B. Kobe, Structural basis and prediction of substrate specificity in protein serine/threonine kinase, Proc. Natl. Acad. Sci. U.S.A. 100 (2003) 74–79.
[35] L.N. Johnson, R.J. Lewis, Structure basis for control by phosphorylation, Chem. Rev. 101 (2001) 2209–2242.
[36] A. Kreegipuu, N. Blom, S. Brunak, PhosphoBase, a database of phosphorylation sites: release 2.0, Nucleic Acids Res. 27 (1999) 237–239. in: http://www.cbs.dtu.dk/databases/PhosphoBase.